# VALIDATION OF AN EFFICIENT CFD-DEM MODEL FOR LARGE SCALE FLUIDIZED BEDS

**Markus BRAUN[1*], Mohan SRINIVASA[2], and Shitanshu GOHEL[2]**

[1] ANSYS Germany GmbH, Birkenweg 14a, 64293 Darmstadt, GERMANY

[2] ANSYS Software Pvt. Ltd., 32/2 Rajiv Gandhi Infotech Park, Pune, 411057, INDIA
*Corresponding author, E-mail address: Markus.Braun@ansys.com

## ABSTRACT

An existing hybrid approach to multiphase flows, based on a multi-fluid representation of the continuous phases and a Lagrangian representation of dispersed phases, was extended by a soft-sphere DEM approach. The new model utilizes the parcel concept from single phase Euler-Lagrangian models and is efficient also for large scale applications in dense particulate flows. Simulations were conducted and discussed for segregation of a bi-disperse particle mixture in a laboratory scale fluidized bed and a large scale fluidized bed. Results are compared to experimental data. The presented work is part of a larger investigation and is still work in progress. Results for the laboratory scale fluidized bed agree well with experimental data. For the large scale fluidized bed this is not yet the case, although it is expected that the parcel based soft-sphere DEM approach is giving similar results as another hybrid approach based on kinetic theory which have been shown earlier.

## NOMENCLATURE

$a$    Gaussian factor
$\boldsymbol{a}$    particle acceleration
$C_D$    drag coefficient
$f$    friction factor
$F_D$    drag factor
$\mathbf{F}$    Force
$\mathbf{g}$    gravitational acceleration
$K_{pq}$    momentum exchange coefficient
$p$    pressure
$Re$    Reynolds number
$t$    time
$p$    pressure
$\mathbf{S}$    source term
$\mathbf{u}$    velocity
$w$    weighting kernel

$\alpha$    volume fraction
$\gamma$    damping factor
$\delta$    overlap
$\rho$    density
$\mu$    dynamic viscosity

## INTRODUCTION

Chemical and petrochemical process industry use gas-solid fluidized beds for applications like drying, coating, catalytic cracking, etc. Improving these processes and understanding the underlying physical phenomena is the main motivation to develop appropriate models for granular-fluid systems. The Eulerian-Eulerian or Multi-Fluid approach has been the main workhorse for such multiphase flow simulations. Consideration of size distributions as they appear in industrial relevant processes requires additional sets of equations including appropriate closing conditions as they appear in population balances. The main drawback of these approaches is the large increase in computational effort to provide appropriate results. In addition a proper modelling of dense packing and underlying collision effects needs to take into account the size distribution as well.

In many instances, the effects of a particle size distribution can be accounted for by the use of an appropriate mean particle size. Such a method would be able to predict the expansion of the bed as well as other gross parameters. However, the amount of fines in fluid catalytic cracking catalysts (FCC) (defined as particles below a size of 45 microns) has a significant impact on the qualitative and quantitative aspects of fluidization of deep beds. When the amount of fines is below a certain threshold, significant by-passing of the gas is observed (Karimipor, 2010 and reference therein). This leads to a poor quality of fluidization with large parts of the bed not fluidized. The addition of a significant amount of fines reduces considerably gas by-passing. In this instance, it seems imperative to include a full description of the particle size distribution rather than just a representative diameter.

In this paper we present an efficient method which is based on the framework of the Dense Discrete Phase Model (Popoff and Braun, 2007), extended by a Discrete Element Method, which makes use of the concept of parcels.

This new model is applied first to simulate segregation of a bi-disperse fluidized bed experiment (Goldschmidt, 2001) and then used to simulate experimental data, published for the NETL challenge 2010 (NETL, 2010).

## MODEL DESCRIPTION

The framework of the Dense Discrete Phase Model consists of several parts: equations for the continuous gas flow, equations describing the dispersed particle flow, and equations coupling both parts. Dispersed phases can be considered as continuous dispersed phases or as discrete dispersed phases. For a continuous dispersed phase a set of partial differential equations is solved in accordance to a multi fluid approach. For a discrete dispersed phase a Lagrangian approach is used and for a set of reference particles a set of ordinary differential equations are solved. This concept allows an adequate mixing of the best suited methods for a specific application.

## Continuous gas phase

The gas phase is modelled in the context of a multi fluid approach, which includes a volume fraction for each phase. The generic equations for a continuous phase p is written as

$$\frac{\partial(\alpha_p \rho_p)}{\partial t} + \nabla \cdot (\alpha_p \rho_p \mathbf{u}_p) = 0 \qquad (1)$$

$$\frac{\partial(\alpha_p \rho_p \mathbf{u}_p)}{\partial t} + \nabla \cdot (\alpha_p \rho_p \mathbf{u}_p \mathbf{u}_p) = -\alpha_p \nabla p$$
$$+ \nabla \cdot [\alpha_p \mu_p (\nabla \mathbf{u}_p + \nabla \mathbf{u}_p^T)] + \alpha_p \rho_p \mathbf{g} \qquad (2)$$
$$+ \sum_q K_{pq} (\mathbf{u}_q - \mathbf{u}_p) + \mathbf{S}_{other}$$

The first equation is the mass conservation equation which does not consider any mass exchange between phases p and q. This would require some additional terms which are omitted for simplicity.

The second equation is the appropriate formulation of change of momentum of a phase p. The summation over all phases in this equation includes the exchange of momentum due to drag between phase p and q, $K_{pq}$. In its generic formulation, momentum exchange due drag can be considered for any continuous or any dispersed phase p with any other phase q. For this application only two phases exist: the continuous phase consisting of air and the disperse particle phase. The last term in equation (2) is considered to account for other source terms which arise from explicit formulations of virtual mass force and pressure force acting on the particles.

### Particle equations

The particle acceleration can be derived from a force balance.

$$\frac{d\mathbf{u}_p}{dt} = F_D(\mathbf{u}_c - \mathbf{u}_p) + \mathbf{g}\left(\frac{\rho_p - \rho_c}{\rho_p}\right)$$
$$+ \mathbf{a}_{vm} + \mathbf{a}_p + \mathbf{a}_{coll} \qquad (3)$$

The first term on the right hand side covers drag effects, while the second term considers gravity. The third and fourth term on the right hand side account for accelerations due to virtual mass effects and pressure force. The last term is computed from additional collision forces acting on the particle.

The drag factor $F_D$ is defined as

$$F_D = \frac{18\mu_c}{\rho_p d_p^2} \frac{C_D \mathrm{Re}_p}{24} \qquad (4)$$

where the drag coefficient $C_D$ is modelled according to Wen and Yu (Wen, 1966) or to Gidaspow (Gidaspow, 1992), which is a combination of Wen and Yu model and the Ergun equation (Ergun, 1952).

The collision forces are computed following the soft sphere approach of Cundall and Strack (Cundall, 1979). This modelling approach has been named in the past Discrete Element Method (DEM). Here, the forces due to particle collision are estimated from the overlap δ between pairs of spheres or between a sphere and a boundary.

$$\mathbf{F}_\delta = (K\delta + \gamma(\mathbf{v}_{12} \cdot \mathbf{e}_{12}))\mathbf{e}_{12} \qquad (5)$$

In addition friction is considered based on the normal force between spheres and a friction factor.

$$\mathbf{F}_f = f\mathbf{F}_n \qquad (6)$$

The friction factor f depends on relative velocity between the particles and includes sticking friction, gliding friction and high velocity friction.

### Representation of particles using parcels

Equations (3) to (6) are valid for every particle. Typically, billions of particles exist in fluidized bed and it is not possible to solve these equations for all particles. Therefore particles are collected into parcels and only a reference particle in each parcel is considered. The number of parcels represents the resolution of the discrete dispersed phase similar to the mesh resolution of a continuous phase. When computing the momentum exchange term $K_{pq}$ as well as any particle related source term the source arising from the reference particle is multiplied by the number of particles in the parcel.

For the DEM method the usage of parcels has also some impact. To evaluate the collision forces $\mathbf{F}_\delta$ and $\mathbf{F}_n$ the mass of the colliding parcels has to be used instead of the mass of the colliding reference particles. For this the parcels are considered to be massive spheres. By this the correct volume fraction of sphere packing is achieved, when parcels are closely packed. For the evaluation of acceleration and drag forces the reference particle diameter $d_p$ is used.

## NUMERICAL SOLUTION PROCEDURE

The sets of equations (1) and (2) are solved within FLUENT R14.5 which is using the Finite Volume approach for an unstructured collocated grid (Mathur, 1997). The multi-fluid formulation is based on the phase coupled SIMPLE approach of Vasquez et. al. (Vasquez, 2000). For this application only the continuous phase of air is discretised with equations (1) and (2). The particulate phase is computed based on the Lagrangian approach represented by equations (3) to (6).

### Coupling of particles with the gas phase

The Lagrangian particles are tracked using an implicit discretisation scheme of equations (3). For the computation of the related source terms a particle source in cell approach is utilized. In every time step the momentum exchange coefficient $K_{pq}$, the particle volume fraction, and the averaged particle velocity components are computed once the new particle locations are known. The momentum exchange coefficient and the drag factor are related to each other via the following equation

$$K_{pq} = \frac{18}{24} \alpha_p \rho_p F_D \qquad (7)$$

Once these values are known in each finite volume cell, equations (1) and (2) are solved in the continuous phase using an iterative approach.

To increase numerical stability and reduce mesh dependency the particle based momentum exchange coefficient $K_{pq}$, the particle volume fraction, and the averaged particle velocity components have been averaged between neighbouring mesh cells. For this a Gaussian

kernel has been implemented (Apte, 2008, and Kaufmann, 2008).

$$w(\Delta x) = \left(\frac{a}{\pi}\right)^{1.5} \exp\left(-a\frac{|\Delta x|^2}{|\Delta x|^2_{cell}}\right) \qquad (8)$$

Here, $\Delta x$ is the distance between the particle location and the neighbouring cell, $\Delta x_{cell}$ is a characteristic length scale of the cell containing the particle, and 'a' is parameter which can be used to control the width of the Gaussian distribution. In all simulations this value was set to 1.

## SEGREGATION OF BIDISPERSE FLOW

Goldschmidt measured segregation of binary mixtures of particles with different diameters in a quasi 2d fluidized bed. He used different mixtures of 1.5mm and 2.5mm glass beads at several superficial velocities and extracted the average height of each diameter class using digital image analysis. The fluidized bed had a size of 0.15m x 0.015m x 0.7m.

From these experiments the set with 50% mass weight of 1.5mm and 2.5mm particle diameters and a superficial velocity of 1.1m/s was simulated with the presented approach.

### Simulation Setup

The domain was discretized using nearly cubic hexahedral cells with a cell count of 47 x 5 x 94 cells. At the bottom a velocity of 1.1m/s was specified for the air. The perforated plate was established by letting the particles reflect at the bottom. The bed content was represented by 33689 Lagrangian parcels filling the bed for 0.075m. Each parcel consisted of exactly one particle. For the collision, the spring dashpot force law was used with a spring constant of 100N/m. Although this is not reflecting the real behaviour of glass beads, it has been shown by Hoomans, that this is a suitable value in combination with an appropriate time step for soft-sphere models (Hoomans, 2000). Simulations have been run for 120s of real time. The center of each particle diameter class has been monitored over time.

### Results

Figure (1) shows the evolution of center of mass for large and small diameter class over time compared to experiments. All simulation data are shown to provide a picture of unsteady behaviour of the different diameter classes. Experimental data have been averaged for a period of 10s. For the small particles the fluctuation is much higher than for the large particles. This is consistent with experimental data of RMS values of the height of the center of mass (Goldschmidt, 2001).
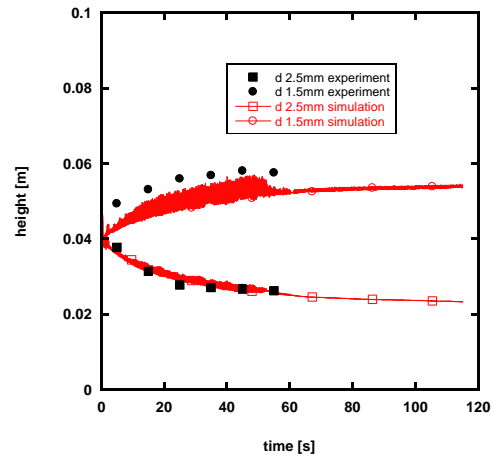


**Figure 1:** Evolution of center of mass over time of a bidisperse mixture

## LARGE SCALE NETL REACTOR

The bubbling fluidized bed reactor used in the 3rd NETL challenge has an inner diameter of 0.9m and a height of 7m. Fluidization air is supplied downwards by a ring sparger, see figure (2). Particles, leaving the fluidized bed at the top, are separated from the gas flow via two cyclones and returned into the bed. Bed material consisted of FCC particles provided by PSRI.

Experimental data have been provided for several cases using two different particle size distributions, two different air distributers, two different superficial gas velocities, and several initial bed heights.
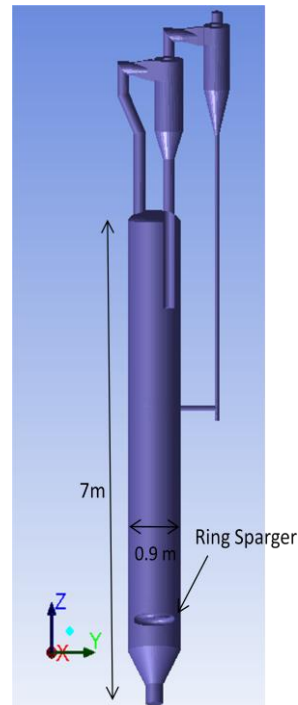


**Figure 2**: Geometry of bubbling fluidized bed

The size distributions of the bed material covers ranges from 10μ to 290μ for the 3% fines material and from 10μ to 155μ for the 12% fines material.

3

Pressure drop measurements along the height of the reactor have been conducted at various locations. In addition local difference pressure measurements were done at 4 circumferential locations. The initial bed height was 2.44m.

**Simulation Setup**

The geometry in figure (2) was discretized with a cut cell mesh consisting of about 94,000 cells and a pure hexahedral mesh of about 50,000 cells. The mesh resolution was chosen to be coarse in order to investigate fast turnaround times as it is necessary for engineering simulations. The bed content was discretized using about 520,000 Lagrangian parcels representing the given size distributions of figure (3). Although the parcels represent varying particle diameters, the number of particles in each parcel was chosen in such a way that the parcel diameter, relevant for the DEM collisions, has been kept constant at a value of 0.015m for all computational parcels. This allowed for a transient time step of 0.0005s, which was used in all simulations. The impact of mesh resolution, parcel resolution, as well as the usage of a constant parcel diameter for the DEM collisions needs to be investigated separately.

Parcels leaving at the exit have been identified and reinjected to keep the mass of the bed material constant during the simulation. By this, the separation effect of the cyclones could be emulated.

With the coarse mesh it was not possible to resolve the small orifices in the original ring sparger. The inlet velocity was adjusted accordingly to provide the superficial gas velocity of 0.6m/s.
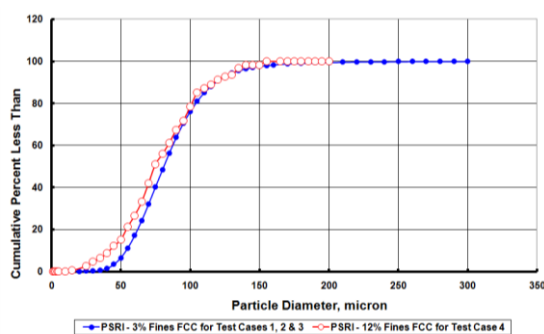


**Figure 3**: Particle size distributions of FCC material.

All simulations have been run for 30s to establish a transient flow field. After that the pressure has been recorded at locations of the experiment and averaged values were sampled for another 20 seconds. In total 100,000 time steps were done.

The simulations have been run in parallel using 8 partitions, giving typical turnaround time of 100 hours of computational time to conduct 50s real time.

**Results**

Results are shown for the size distribution consisting of 3% fines.

First, simulations were carried out for the 50k hexahedral mesh using Wen Yu drag model and a spring constant of 5000 N/m. Figures 4 to 6 give some impression of the established flow field inside the reactor. The fluidization air is entering at the sparger (black area in the pictures). The bed material below the ring sparger is not fluidized and has nearly zero velocity.
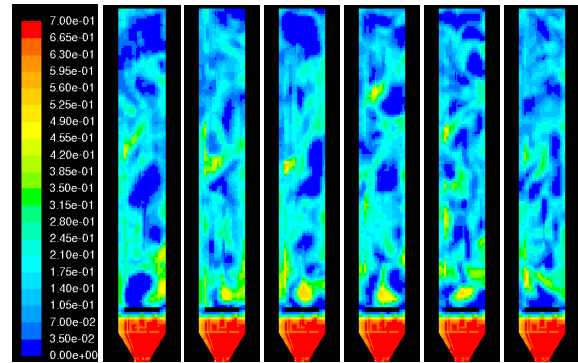


**Figure 4**: FCC volume fractions for 30s, 30.5s, 31s, 31.5s, 32s, and 32.5s (from left to right).

Fluidization air is forming large bubbles and rising the bed material. In areas of low FCC material the air has the highest speed of up to 7 m/s. In particular at the exit (Figure 5, top left), the air velocity magnitude is always more than 7 m/s due to the small cross section of the exit tube.

The FCC material is following the fluidization air at a reduced speed (Figure 6). The transient flow patterns look very similar.
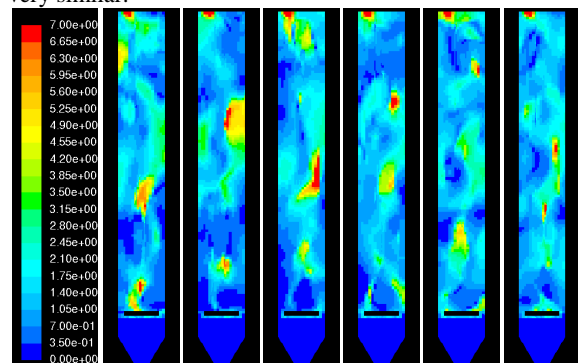


**Figure 5**: Air velocity magnitude for 30s, 30.5s, 31s, 31.5s, 32s, and 32.5s (from left to right).
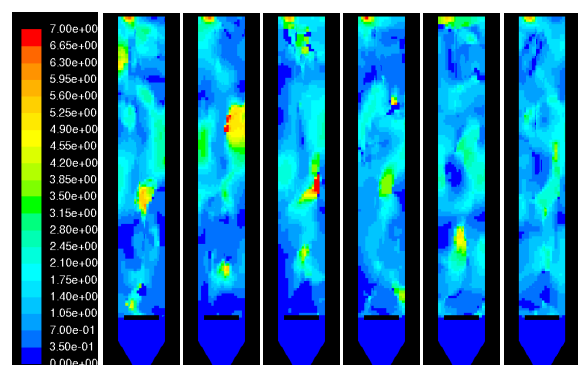


**Figure 6**: FCC velocity magnitude for 30s, 30.5s, 31s, 31.5s, 32s, and 32.5s (from left to right).

In general it looks like the bed is too much expanded, the maximum volume fraction in the fluidized area of the bed is typically not larger than 45%.

Averaged values of the volume fraction, air and FCC velocity magnitude confirm this assessment (Figure 7).
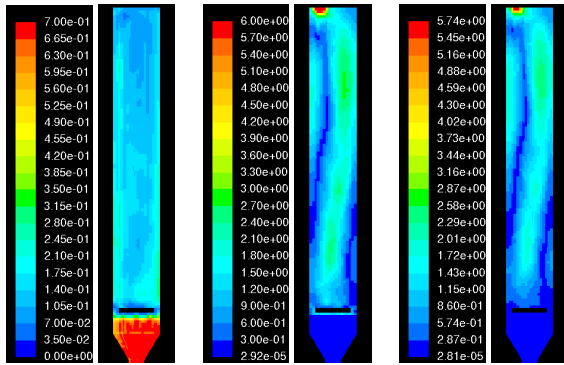
**Figure 7**: Averaged fields of FCC volume fraction (left), air velocity magnitude (middle), FCC velocity magnitude (right).

NETL provided experimental data of pressure drop divided by gravity and distance between pressure devices. In the simulations, the average pressure has been recorded on planes at the appropriate z-coordinates for the last 20 seconds. The time averaged pressure has been used to estimate the local pressure drop (Figure 8).
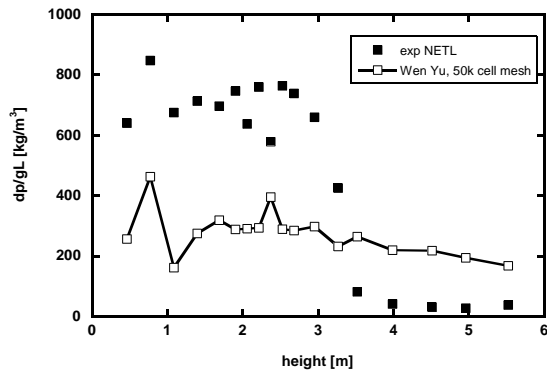


**Figure 8**: Pressure drop per gravity and length unit.

The experimental data indicate that the bed expands to about 3.5m above the sparger, while the simulation results confirm that the bed expands up to the top of the reactor. These results motivated us to further investigation of this behaviour. For this two more simulations were conducted using Gidaspow's drag model and using a finer mesh with 94k cells.
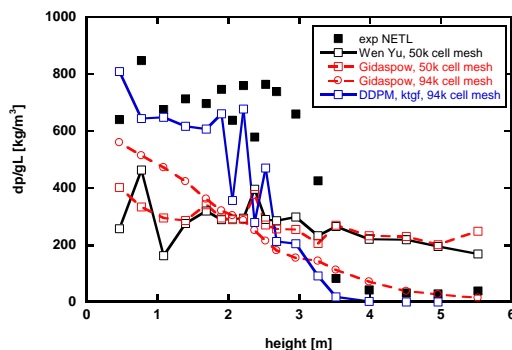


**Figure 9**: Influence of drag law model and mesh resolution on pressure drop per gravity and length unit.

Using Gidaspow's drag model a smooth distribution of the pressure drop is achieved, but the bed expansion still does not match the experiments. Increasing the mesh resolution

gives a better prediction of the pressure drop in the lower part of the reactor. In prior investigations the same case has been simulated using the DDPM framework using kinetic theory of granular flows (blue line in Figure 9). Here the bed expansion was slightly under predicted (Ozarkar, 2011).

**CONCLUSION**

Simulation of segregation of a bi-disperse particle mixture in a laboratory scale fluidized bed gave good agreement with experimental results of the height of center of mass using the presented soft-sphere DEM approach.

For the large scale fluidized bed the presented results do not yet compare well with experimental observation although prior results using the DDPM framework in combination with kinetic theory of granular flows gave satisfying results for the bed expansion even for coarse meshes. Variation of the mesh resolution indicates that the mesh has a more prominent impact than observed previously. Increasing the mesh resolution is subject to current investigations to better understand the connection of mesh resolution and soft-sphere collision modelling. Therefore the results for the large scale fluidized bed are a snapshot of current work in progress.

**REFERENCES**

APTE, S. V., MAHESH, K., and LUNDGREN, L. (2008), "Accounting for finite-size effects in simulations of dispersed particle-laden flows", *Int. J. Multiphase Flows*, **34**, 260-271.

CUNDALL, P. A., and STRACK, O. D. L. (1979), "A Discrete Numerical Model for Granular Assemblies", *Geotechnique*, **29**, 47-65.

ERGUN, S. (1952), "Fluid Flow through Packed Columns", *Chem. Eng. Prog*, **48**, 89-94.

GIDASPOW, D., BEZBURUAH, R., DING, J. (1992), "Hydrodynamics of Circulating Fluidized Beds, Kinetic Theory Approach", in *Fluidization VII, Proc. Of the 7th Engineering Foundation Conference on Fluidization*, 75-82.

GOLDSCHMIDT, M., (2001), "Hydrodynamic Modelling of Fluidised Bed Spray Granulation", PhD Thesis, University of Twente.

HOOMANS, B., (2000), "Granular Dynamics of Gas-Solid Two-Phase Flows", PhD Thesis, University of Twente.

KARIMIPOR, S, (2010), "A study of gas streaming in deep fluidized beds", PhD Thesis, University of Saskatchewan.

KAUFMANN, A., MOREAU, M., SIMONIN, O., HELIE, J. (2008), "Comparison between Lagrangian and meso-scopic Eulerian modelling approaches for inertial particles suspended in decaying isotropic turbulence", *J Comp. Physics*, **13**, 6448-6472.

MATHUR, S., MURTHY, J. (1997), "A Pressure Based Method for Unstructured Meshes", *Numer. Heat Transfer*, **31**, 195-216.

NETL (2010), "NETL/PSRI Challenge Problem 3", https://mfix.netl.doe.gov/challenge/index.php.

OZARKAR, S., SANYAL, J., LIU, F., SRINIVASA, M. (2011), "Comparison of Three Numerical Approaches for Modeling Poly-Disperse Dense Particulate Flows.", *NETL 2011 Workshop on Multiphase Flow Science*, Morgantown, USA, 16-18 August 2011.

POPOFF, B. and BRAUN, M., (2007), "A Lagrangian Approach to Dense Particulate Flows", *6th International*

*Conference on Multiphase Flows*, Leipzig, Germany, July 2007.

VASQUEZ, S., and IVANOV, V. (2000), "A Phase Coupled Method for Solving Multiphase Problems on Unstructured Meshes", *Proceedings of the ASME FEDSM'00: ASME 2000 Fluids engineering Division Summer Meeting*, Boston, 2000.

WEN, C.-Y., and YU, Y. H. (1966), "Mechanics of Fluidization", *Chem. Eng. Prog. Symp. Series*, **62**, 100-111.